TITLE

Ilia Kohanovski[a], Uri Obolski[b,c], and Yoav Ram[a,*]

[a]School of Computer Science, Interdisciplinary Center Herzliya, Herzliya 4610101, Israel
[b]School of Public Health, Tel Aviv University, Tel Aviv 6997801, Israel
[c]Porter School of the Environment and Earth Sciences, Tel Aviv University, Tel Aviv 6997801, Israel
[*]Corresponding author: yoav@yoavram.com

May 3, 2020

Abstract

Lorem ipsum dolor sit amet, consectetuer adipiscing elit. Ut purus elit, vestibulum ut, placerat ac, adipiscing vitae, felis. Curabitur dictum gravida mauris. Nam arcu libero, nonummy eget, consectetuer id, vulputate a, magna. Donec vehicula augue eu neque. Pellentesque habitant morbi tristique senectus et netus et malesuada fames ac turpis egestas. Mauris ut leo. Cras viverra metus rhoncus sem. Nulla et lectus vestibulum urna fringilla ultrices. Phasellus eu tellus sit amet tortor gravida placerat. Integer sapien est, iaculis in, pretium quis, viverra ac, nunc. Praesent eget sem vel leo ultrices bibendum. Aenean faucibus. Morbi dolor nulla, malesuada eu, pulvinar at, mollis ac, nulla. Curabitur auctor semper nulla. Donec varius orci eget risus. Duis nibh mi, congue eu, accumsan eleifend, sagittis quis, diam. Duis eget orci sit amet orci dignissim rutrum.

Introduction

The COVID-19 pandemic has resulted in implementation of extreme non-pharmaceutical interventions (NPIs) in many affected countries. These interventions, from social distancing to lockdowns, are applied in a rapid and widespread fashion. The NPIs are designed and assessed using epidemiological models, which follow the dynamics of the viral infection to forecast the effect of different mitigation and suppression strategies on the levels of infection, hospitalization, and fatality. These epidemiological models usually assume that the effect of NPIs on disease transmission begins at the officially declared date (e.g. Flaxman et al.[5], Gatto et al.[7], Li et al.[9]).

Adoption of public health recommendations is often critical for effective response to infectious diseases, and has been studied in the context of HIV[8] and vaccination[3,12], for example. However, behavioral and social change does not occur immediately, but rather requires time to diffuse in the population through media, social networks, and social interactions. Moreover, compliance to NPIs may differ between different interventions and between people. For example, in a survey of 2,108 adults in the UK during Mar 2020, Atchison et al.[2] found that those over 70 years old were more likely to adopt social distancing than young adults (18-34 years old), and that those with lower income were less likely to be able to work from home and to self-isolate. Furthermore, compliance to NPIs may be impacted by risk perception, as percieved by the number of domestic cases or even by reported cases in other regions and countries. Interestingly, the perceived risk of COVID-19 infection has likely caused a reduction in the number of influenza-like illness cases in the US starting from mid-February[13].

Here, we hypothesize that there is a significant difference between the official start of NPIs and their adoption by the public and therefore their effect on transmission dynamics. We use a *Susceptible-Exposed-Infected-Recovered* (SEIR) epidemiological model and *Markov Chain Monte Carlo* (MCMC) parameter estimation framework to estimate the effective start date of NPIs from publicly available COVID-19 case data in several geographical regions. We compare these estimates to the official dates and find both delayed and advanced effect of NPIs on COVID-19 transmission dynamics. We conclude by demonstrating how differences between the official and effective start of NPIs can confuse assessments of the effectiveness of the NPIs in a simple epidemic control framework.

Models and Methods

Data. We use daily confirmed case data $\mathbf{X} = (X_1, \ldots, X_T)$ from several different countries. These incidence data summarize the number of individuals X_t tested positive for SARS-CoV-2 RNA (using RT-qPCR) at each day t. Data was retrieved for X regions, see Table 1 for details and references. In regions in which there were multiple sequences of days with zero confirmed cases (e.g. France), we cropped the data to begin with the last sequence so that our analysis focuses on the first sustained outbreak rather than isolated imported cases.

Region	Start date	End date	Reference
Austria	X Feb		Flaxman et al.[5]
Wuhan, China	10 Jan	8 Feb	Pei and Shaman[10]

Table 1: Reference for confirmed cases incidence data. All dates in 2020.

SEIR model. We model SARS-CoV-2 infection dynamics by following the number of susceptible S, exposed E, reported infected I_r, and unreported infected I_u individuals in a population of size N. This model distinguishes between reported and unreported infected individuals: the reported infected

are those that have enough symptoms to eventually be tested and thus appear in daily case reports, to which we fit the model.

Susceptible (S) individuals become exposed due to contact with reported or unreported infected individuals (I_r or I_u) at a rate β_t or $\mu\beta_t$. The parameter $0 < \mu < 1$ represents the decreased transmission rate from unreported infected individuals, who are often subclinical or even asymptomatic. The transmission rate $\beta_t \geq 0$ may change over time t due to behavioural changes of both susceptible and infected individuals. Exposed individuals, after an average incubation period of Z days, become reported infected with probability α_t or unreported infected with probability $(1 - \alpha_t)$. The reporting rate $0 < \alpha_t < 1$ may also change over time due to changes in human behavior. Infected individuals remain infectious for an average period of D days, after which they either recover, or becomes ill enough to be quarantined. They therefore no longer infect other individuals, and the model does not track their frequency. The model is described by the following equations:

$$\begin{aligned}
\frac{dS}{dt} &= -\beta_t S\frac{I_p}{N} - \mu\beta_t S\frac{I_s}{N} \\
\frac{dE}{dt} &= \beta_t S\frac{I_p}{N} + \mu\beta_t S\frac{I_s}{N} - \frac{E}{Z} \\
\frac{dI_r}{dt} &= \alpha_t\frac{E}{Z} - \frac{I_r}{D} \\
\frac{dI_u}{dt} &= (1-\alpha_t)\frac{E}{Z} - \frac{I_r}{D}.
\end{aligned} \tag{1}$$

The initial numbers of exposed $E(0)$ and unreported infected $I_u(0)$ are considered model parameters, whereas the initial number of reported infected is assumed to be zero $I_r(0) = 0$, and the number of susceptible is $S(0) = N - E(0) - I_u(0)$. The vector θ of model parameters is

$$\theta = \Big(Z, D, \mu, \{\beta_t\}, \{\alpha_t\}, \{p_t\}, E(0), I_u(0)\Big). \tag{2}$$

This model is inspired by Li et al.[9] and Pei and Shaman[10], who used a similar model with multiple regions and constant transmission β and reporting rate α to infer COVID-19 dynamics in China and the continental US, respectively.

Likelihood function. The *expected* cumulative number of reported infected individuals until day t is

$$Y_t = \int_0^t \alpha_s\frac{E(s)}{Z}\,ds, \quad Y_0 = 0. \tag{3}$$

We assume that reported infected individuals are confirmed and therefore observed in the daily case report of day t with probability p_t (note that an individual can only be observed once, and that p_t may change over time, but t is a specific date rather than the time elapsed since the individual was infected). Hence, we assume that the number of confirmed cases in day t is binomially distributed,

$$X_t \sim Bin\big(n_t, p_t\big),$$

where n_t is the *realized* (rather than expected) number of reported infected individuals yet to appear in daily reports by day t. The cumulative number of confirmed cases until day t is

$$\tilde{X}_t = \sum_{i=1}^{t} X_i, \quad X_0 = 0.$$

Given $\tilde{X}_{t-1}$, we assume n_t is Poisson distributed,

$$\big(n_t \mid \tilde{X}_{t-1}\big) \sim Poi\Big(Y_t - \tilde{X}_{t-1}\Big), \quad n_1 \sim Poi(Y_1).$$

Therefore, $\left(X_t \mid \tilde{X}_{t-1}\right)$ is a binomial conditioned on a Poisson, which reduces to a Poisson with

$$\left(X_t \mid \tilde{X}_{t-1}\right) \sim Poi\Big(\left(Y_t - \tilde{X}_{t-1}\right) \cdot p_t\Big), \quad X_1 \sim Poi(Y_1 \cdot p_1). \tag{4}$$

For given vector θ of model parameters (Eq. (2)), we compute the expected cumulative number of reported infected individuals $\{Y_t\}_{t=1}^{T}$ for each day (Eq. (3)). Then, since $\tilde{X}_{t-1}$ is a function of $X_1, \ldots, X_{t-1}$, we can use Eq. (4) to write the probability to observe the confirmed case data $\mathbf{X} = (X_1, \ldots, X_T)$ as

$$\mathbb{L}(\theta \mid \mathbf{X}) = P(\mathbf{X} \mid \theta) = P(X_1 \mid \theta) P(X_2 \mid \tilde{X}_1, \theta) \cdots P(X_T \mid \tilde{X}_{T-1}, \theta). \tag{5}$$

This defines a *likelihood function* $\mathbb{L}(\theta \mid \mathbf{X})$ for the parameter vector θ given the data $\mathbf{X}$.

NPI model. To model non-pharmaceutical interventions (NPIs), we set the beginning of the NPIs to day τ and define

$$\beta_t = \begin{cases} \beta, & t < \tau \\ \beta\lambda, & t \geq \tau \end{cases}, \quad \alpha_t = \begin{cases} \alpha_1, & t < \tau \\ \alpha_2, & t \geq \tau \end{cases}, \quad p_t = \begin{cases} 1/9, & t < \tau \\ 1/6, & t \geq \tau \end{cases}, \tag{6}$$

where $0 < \lambda < 1$. The values for p_t follow Li et al.[9], who estimated the average time between infection and reporting in Wuhan, China, at 9 days before the start of NPIs (Jan 23, 2020) and 6 days after start of NPIs. The parameter τ is then added to the parameter vector θ (Eq. (2)).

Parameter estimation. To estimate the parameters θ of our model (Eq. (1)) from the data $\mathbf{X}$, we apply a Bayesian inference approach. We define the following flat priors on the model parameters $P(\theta)$:

$$\begin{aligned} Z &\sim Uniform(2, 5) \\ D &\sim Uniform(2, 5) \\ \mu &\sim Uniform(0.2, 1) \\ \beta &\sim Uniform(0.8, 1.5) \\ \lambda &\sim Uniform(0, 1) \\ \alpha_1, \alpha_2 &\sim Uniform(0.02, 1) \\ E(0) &\sim Uniform(0, 3000) \\ I_u(0) &\sim Uniform(0, 3000) \\ \tau &\sim Uniform(1, T-1), \end{aligned} \tag{7}$$

where T is the number of days in the data $\mathbf{X}$. Most priors follow Li et al.[9], except λ, which is used to enforce that the transmission rates are lower after the start of the NPIs ($\lambda < 1$). The likelihood function is defined in Eq. (5). The posterior distribution on the model parameters $P(\theta \mid \mathbf{X})$ is then estimated using an *affine-invariant ensemble sampler for Markov chain Monte Carlo* (MCMC) implemented in the `emcee` Python package[6].

Model selection. We perform model selection using DIC (deviance information criterion)[11],

$$\begin{aligned} DIC(\theta, \mathbf{X}) &= 2\mathbb{E}[D(\theta)] - D(\mathbb{E}[\theta]) \\ &= 2 \log \mathcal{L}(\mathbb{E}[\theta] \mid \mathbf{X}) - 4\mathbb{E}[\log \mathcal{L}(\theta \mid \mathbf{X})], \end{aligned} \tag{8}$$

where $D(\theta)$ is the Bayesian deviance, and expectations $\mathbb{E}[\cdot]$ are taken over the posterior distribution $P(\theta \mid \mathbf{X})$. We compare models by reporting their relative DIC; lower is better.

Source code. We use Python 3 (Anaconda) with the NumPy, Matplotlib, SciPy, Pandas, Seaborn, and emcee packages. All source code will be publicly available under a permissive open-source license at github.com/yoavram-lab/EffectiveNPI.

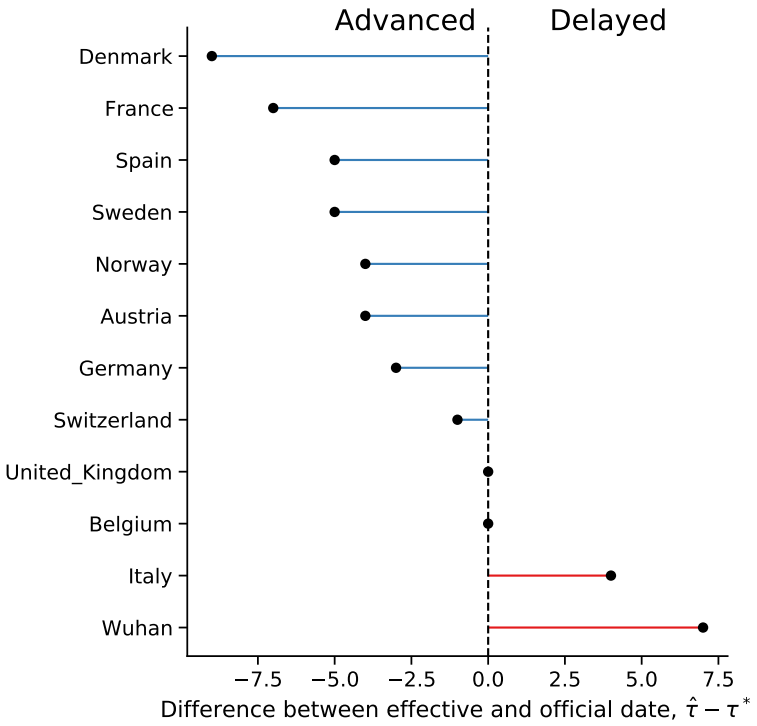

Figure 1: Official and effective start of non-pharmaceutical interventions.

Results

Several studies have described the effects of non-pharmaceutical interventions in different geographical regions[5,7,9]. These studies have assumed that the parameters of the epidemiological model change at a specific date, as in Eq. (6), and set the change date τ to the official NPI date τ^*. They then fit the model once for time $t < \tau^*$ and once for time $t \geq \tau^*$ (see TABLE2 for a summary of official NPI dates.) For example, Li et al.[9] estimate the dynamics in China before and after τ^* at Jan 23. Thereby, they effectively estimate (β, α_1) and (λ, α_2) separately. Here we estimate the posterior distribution $P(\tau \mid \mathbf{X})$ of the *effective* start date of the NPIs by jointly estimating $\tau, \beta, \lambda, \alpha_1, \alpha_2$ on the entire data per region (e.g. Italy, Austria), rather than splitting the data at τ^*. We then compute the maximum a posteriori estimate $\hat{\tau} = argmax_\tau P(\tau \mid \mathbf{X})$.

We find that a model that considers an NPI (Eq. (6)) is a better fit to the data than a model without an NPI, i.e. with constant β and α ($\Delta DIC >?$ for all regions.) We compare the official τ^* and effective $\hat{\tau}$ start of NPIs and find that in most regions the effective start of NPI significantly differs from the official date (Figure 1): the 75% confidence interval on $\hat{\tau}$ does not include τ^*, and the DIC of the model with free τ parameter is lower than that of a model with a fixed $\tau \equiv \tau^*$ ($\Delta DIC >?$.) The exception that proves the rule is Switzerland.

In the following, we describe our findings on delayed and advanced start of NPI in detail.

Delayed effective start of NPI. In both Wuhan, China, and in Italy we find that our estimated effective start of NPI $\hat{\tau}$ is significantly later than the official date τ^* (Figure 1).

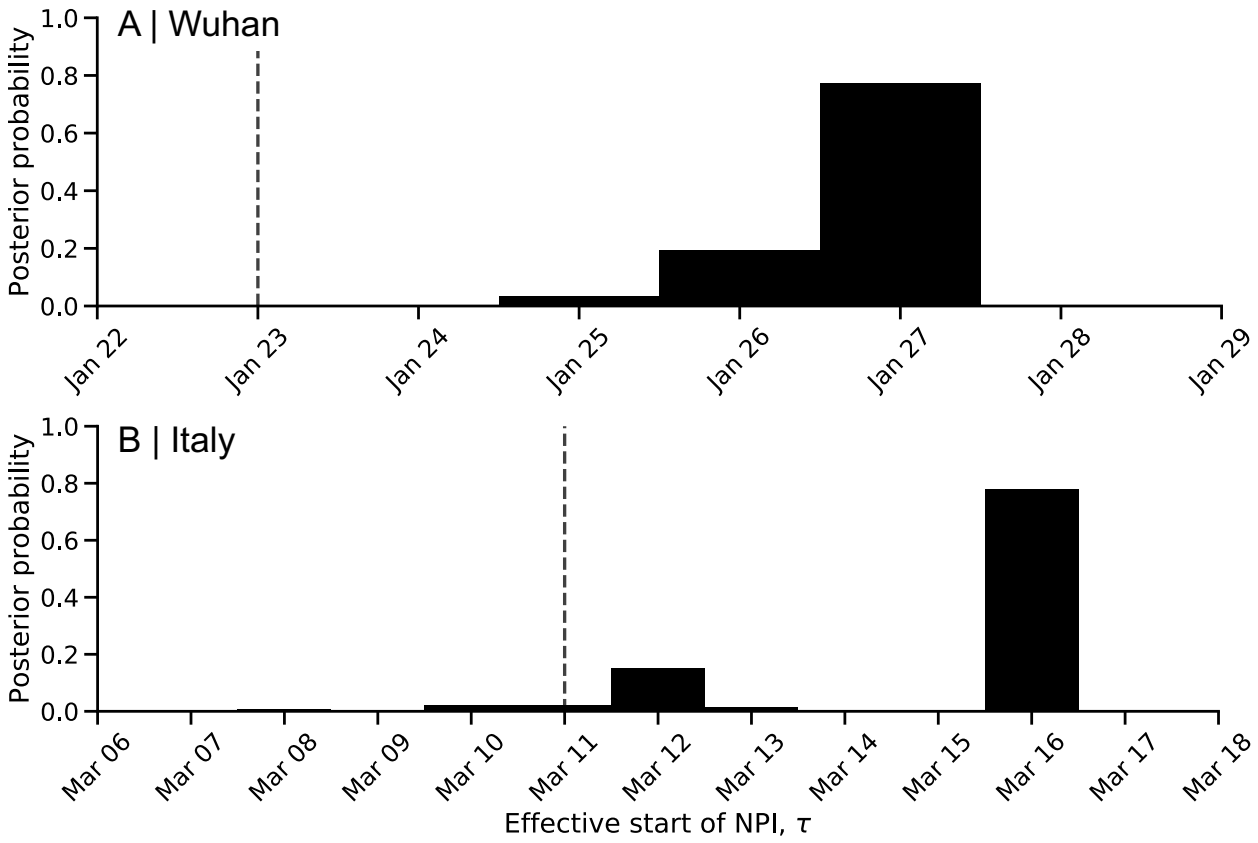

Figure 2: Delayed effect of non-pharmaceutical interventions in Italy and Wuhan, China.

In Italy, the first case officially confirmed on Feb 21, a lockdown was declared in Northern Italy on Mar 8, with social distancing implemented in the rest of the country, and the lockdown was extended to the entire nation on Mar 11[7]. That is, the official date τ^* is either Mar 8 or 11. However, we estimate the effective date $\hat{\tau}$ at Mar 16 (the posterior probability that τ is later than Mar 11 is $(P(\tau > \tau^*) = ???)$ (Figure 2). Similarly, in Wuhan, China, lockdown was declared on Jan 23[9], but we estimate the effective start of NPIs to be 3-4 days layer $(P(\tau > \tau^*) = ???)$ (Figure 2).

Advanced effective start of NPIs. In contrast, in some regions we estimate an effective start of NPIs $\hat{\tau}$ that is *earlier* then the official date τ^* (Figure 1). For example, in Spain social distancing was encouraged starting on Mar 8[5], but mass gatherings still occurred on Mar 8, including a march of 120,000 people for the International Women's Day, and a football match between Real Betis and Real Madrid (2:1) with a crowd of 50,965 in Seville. A national lockdown was only announced on Mar 14[5]. Nevertheless, we estimate the effective start of NPI $\hat{\tau}$ at Mar 8 or 9, rather than Mar 14 $(P(\tau < \tau^*) = ???)$ (Figure 3).

The exception that proves the rule. We find one case in which the official and effective dates match: Switzerland ordered a national lockdown on Mar 20, after banning public evens and closing schools on Mar 13 and 14[5]. Indeed, our MAP estimate $\hat{\tau}$ is Mar 20, and the posterior distribution shows two density peaks: a smaller one between Mar 10 and Mar 14, and a taller one between Mar 17 and Mar 22. It's also worth mentioning that Switzerland was the first to mandate self isolation of confirmed cases[5].

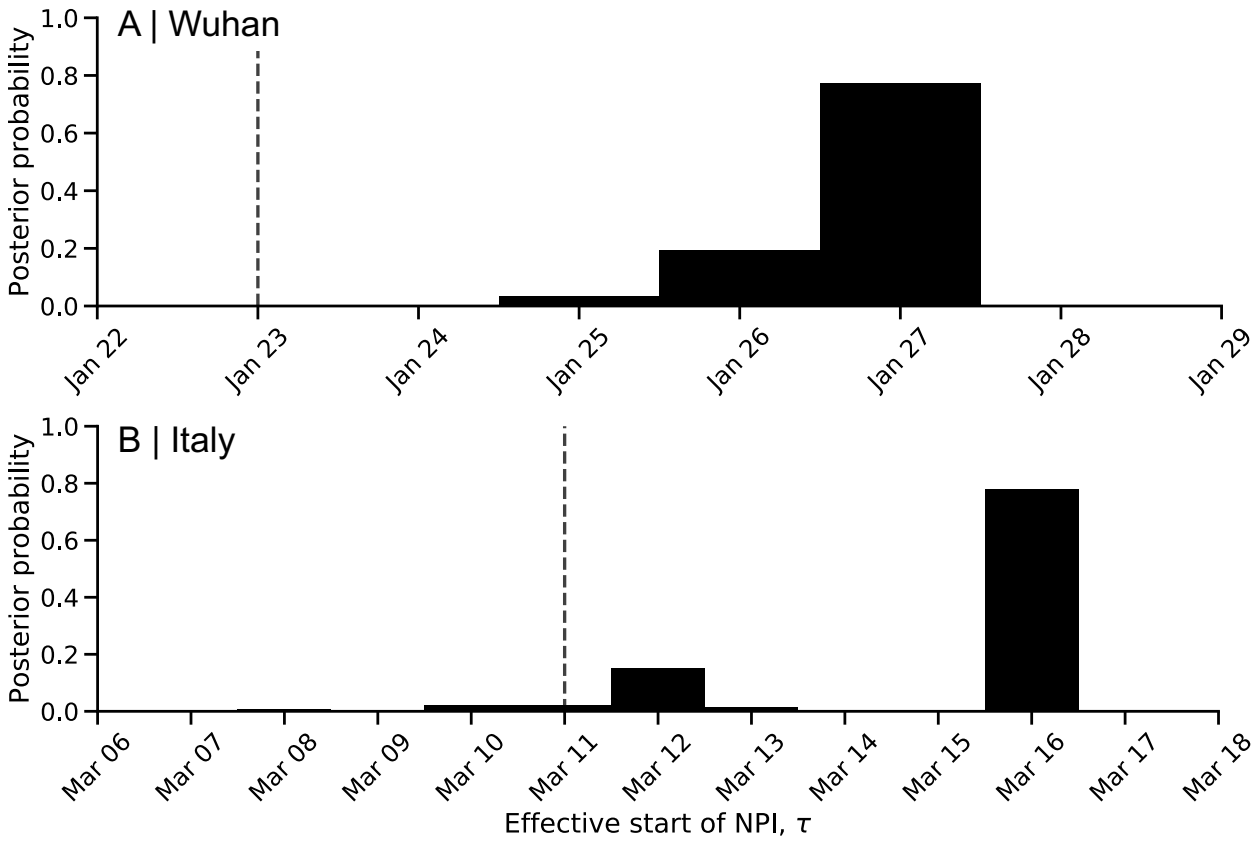

Figure 3: Advanced effect of non-pharmaceutical interventions in Spain and France.

Effect of delays and advances of real-time assessment. The success of non-pharmaceutical interventions is assessed by health officials using various metrics, such as the decline in the growth rate of daily cases. These assessments are made a specific number of days after the intervention began, to accommodate for the expected serial interval (i.e. time between successive cases in a chain of transmission), which is estimated at about 4-7 days[7]. However, we hypothesize that a significant difference between the beginning of the intervention and the effective change in transmission rates invalidates assessments that assume 4-7 days. What are good metrics for assessment of intervention success? growth rate of daily cases, hospitalisations, deaths?

Discussion

We have estimated the effective start date of NPIs in several geographical regions using an SEIR epidemiological model and an MCMC parameter estimation framework. We find examples of both advanced and delayed response to NPIs (Figure 1).

For example, in Italy and Wuhan, China, the effective start of the lockdowns seems to have occurred 3-5 after the official date (Figure 2). This could be explained by low compliance. In Italy, for example, a leak about the intent to lockdown Northern provinces results in people leaving those provinces[7]. However, delayed effect of NPIs could also be due to the time required by both the government and the citizens to organize for a lockdown.

In contrast, in other countries, such as Spain and France, transmission rates seem to have been reduced even before official lockdowns were implemented (Figure 3). This advanced response is possibly due to adoption of social distancing and similar behavioral adaptations in parts of the population, maybe in response increased risk perception due to domestic or international COVID-19-related reports.

As several countries (e.g. Austria, Israel) have began to relieve lockdowns and ease restrictions, we expect similar delays and advances to occur: in some countries people will begin to behave as if restrictions were eased even before the official date, and in some countries people will continue to self-restrict even after restrictions are officially removed. Such delays and advances could confuse analyses and lead to wrong conclusions about the effects of NPI removals.

Conclusions. We have estimated the effective start date of NPIs and found that they often differ from the official dates. Our results emphasize the complex interaction between personal, regional, and global determinants of behavioral. Thus, our results highlight the need to further study variability in compliance and behavior over both time and space. This can be accomplished both by surveying differences in compliance within and between populations[2], and by incorporating specific behavioral models into epidemiological models[1,4].

Acknowledgements

This work was supported in part by the Israel Science Foundation 552/19 (YR) and XXX/XX (Alon Rosen).

References

[1] Arthur, R. F., Jones, J. H., Bonds, M. H. and Feldman, M. W. 2020, 'Complex dynamics induced by delayed adaptive behavior during outbreaks', *bioRxiv* pp. 1–23.

[2] Atchison, C. J., Bowman, L., Vrinten, C., Redd, R., Pristera, P., Eaton, J. W. and Ward, H. 2020, 'Perceptions and behavioural responses of the general public during the COVID-19 pandemic: A cross-sectional survey of UK Adults', *medRxiv* p. 2020.04.01.20050039.

[3] Dunn, A. G., Leask, J., Zhou, X., Mandl, K. D. and Coiera, E. 2015, 'Associations between exposure to and expression of negative opinions about human papillomavirus vaccines on social media: An observational study', *J. Med. Internet Res.* **17**(6), e144.

[4] Fenichela, E. P., Castillo-Chavezb, C., Ceddiac, M. G., Chowellb, G., Gonzalez Parrae, P. A., Hickling, G. J., Holloway, G., Horan, R., Morin, B., Perrings, C., Springborn, M., Velazquez, L. and Villalobos, C. 2011, 'Adaptive human behavior in epidemiological models', *Proc. Natl. Acad. Sci. U. S. A.* **108**(15), 6306–6311.

[5] Flaxman, S., Mishra, S., Gandy, A., Unwin, J. T., Coupland, H., Mellan, T. A., Zhu, H., Berah, T., Eaton, J. W., Guzman, P. N. P., Schmit, N., Cilloni, L., Ainslie, K. E. C., Baguelin, M., Blake, I., Boonyasiri, A., Boyd, O., Cattarino, L., Ciavarella, C., Cooper, L., Cucunubá, Z., Cuomo-Dannenburg, G., Dighe, A., Djaafara, B., Dorigatti, I., Van Elsland, S., Fitzjohn, R., Fu, H., Gaythorpe, K., Geidelberg, L., Grassly, N., Green, W., Hallett, T., Hamlet, A., Hinsley, W., Jeffrey, B., Jorgensen, D., Knock, E., Laydon, D., Nedjati-Gilani, G., Nouvellet, P., Parag, K., Siveroni, I., Thompson, H., Verity, R., Volz, E., Gt Walker, P., Walters, C., Wang, H., Wang, Y., Watson, O., Xi, X., Winskill, P., Whittaker, C., Ghani, A., Donnelly, C. A., Riley, S., Okell, L. C., Vollmer, M. A. C., Ferguson, N. M. and Bhatt, S. 2020, 'Estimating the number of infections and the impact of non-pharmaceutical interventions on COVID-19 in 11 European countries', *Imp. Coll. London* (March), 1–35.

[6] Foreman-Mackey, D., Hogg, D. W., Lang, D. and Goodman, J. 2013, 'emcee : The MCMC Hammer ', *Publ. Astron. Soc. Pacific* **125**(925), 306–312.

[7] Gatto, M., Bertuzzo, E., Mari, L., Miccoli, S., Carraro, L., Casagrandi, R. and Rinaldo, A. 2020, 'Spread and dynamics of the COVID-19 epidemic in Italy: Effects of emergency containment measures', *Proc. Natl. Acad. Sci.* p. 202004978.

[8] Kaufman, M. R., Cornish, F., Zimmerman, R. S. and Johnson, B. T. 2014, 'Health behavior change models for HIV prevention and AIDS care: Practical recommendations for a multilevel approach', *J. Acquir. Immune Defic. Syndr.* **66**(SUPPL.3), 250–258.

[9] Li, R., Pei, S., Chen, B., Song, Y., Zhang, T., Yang, W. and Shaman, J. 2020, 'Substantial undocumented infection facilitates the rapid dissemination of novel coronavirus (SARS-CoV2)', *Science (80-.).* p. eabb3221.

[10] Pei, S. and Shaman, J. 2020, 'Initial Simulation of SARS-CoV2 Spread and Intervention Effects in the Continental US', *medRxiv* p. 2020.03.21.20040303.

[11] Spiegelhalter, D. J., Best, N. G., Carlin, B. P. and Van Der Linde, A. 2002, 'Bayesian measures of model complexity and fit', *J. R. Stat. Soc. Ser. B Stat. Methodol.* **64**(4), 583–616.

[12] Wiyeh, A. B., Cooper, S., Nnaji, C. A. and Wiysonge, C. S. 2018, 'Vaccine hesitancy âĂŸoutbreaks': using epidemiological modeling of the spread of ideas to understand the effects of vaccine related events on vaccine hesitancy', *Expert Rev. Vaccines* **17**(12), 1063–1070.

[13] Zipfel, C. M. and Bansal, S. 2020, 'Assessing the interactions between COVID-19 and influenza in the United States', *medRxiv* (February), 1–13.